Potential environmental impact of bromoform from Asparagopsis farming in Australia

Yue Jia[1, a], Birgit Quack[2*], Robert D. Kinley[3], Ignacio Pisso[4], Susann Tegtmeier[1]

[1] Institute of Space and Atmospheric Studies, University of Saskatchewan, Saskatoon, Canada

[2] GEOMAR Helmholtz Centre for Ocean Research Kiel, Kiel, Germany

[3] Commonwealth Scientific and Industrial Research Organisation (CSIRO), Agriculture and Food, Townsville, QLD, Australia

[4] Norwegian Institute for Air Research (NILU), Kjeller, Norway

[a] *now at*: Cooperative Institute for Research in Environmental Sciences (CIRES), University of Colorado Boulder, Boulder, CO, USA.

**Corresponding to*: B. Quack (bquack@geomar.de)

Abstract

To mitigate the rumen enteric methane (CH_4) produced by ruminant livestock, *Asparagopsis taxiformis* is proposed as an additive to ruminant feed. During the cultivation of *Asparagopsis taxiformis* in the sea or in terrestrial based systems, this macroalgae, like most seaweeds and phytoplankton, produces a large amount of bromoform ($CHBr_3$), which contributes to ozone depletion once released into the atmosphere. In this study, we focus on the impact of $CHBr_3$ on the stratospheric ozone layer resulting from potential emissions from proposed *Asparagopsis* cultivation in Australia. The impact is assessed by weighting the emissions of $CHBr_3$ with its ozone depletion potential (ODP), which is traditionally defined for long-lived halocarbons but has been also applied to very short-lived substances (VSLSs). An annual yield of ~3.5×10^4 Mg dry weight is required to meet the needs of 50% of the beef feedlot and dairy cattle in Australia. Our study shows that the intensity and impact of $CHBr_3$ emissions varies, depending on location and cultivation scenarios. Of the proposed locations, tropical farms near the Darwin region are associated with largest $CHBr_3$ ODP values. However, farming of Asparagopsis using either ocean or terrestrial cultivation systems at any of the proposed locations does not have potential to significantly impact the ozone layer. Even if all *Asparagopsis* farming was performed in Darwin, the $CHBr_3$ emitted into the atmosphere would amount to less than 0.02% of the global ODP-weighted emissions. The impact of remaining farming scenarios is also relatively small even if the intended annual yield in Darwin is scaled by a factor 30 to meet the global requirements, which will increase the global ODP-weighted emissions up to ~0.5%

1. Introduction

Livestock is responsible for about 15% total anthropogenic greenhouse gas (GHG) emissions weighted by radiative forcing (Gerber et al., 2013), ranking it amongst the main contributors to climate change. The global demand for red meat and dairy is expected to increase >50% by 2050 compared to 2010 level, thus mitigation measures to reduce the GHG emissions from the global livestock industry are in high demand (Beauchemin et al., 2020). Total GHG emissions (e.g., CH_4) from ruminant livestock contribute about 18% of the total global carbon dioxide equivalent (CO_2-eq) inventory (Herrero and Thornton, 2013). With a global warming potential ~30 times higher than carbon dioxide (CO_2) and a much shorter lifetime (~10 years, IPCC, 2021), ruminant enteric CH_4 is an attractive and feasible target for global warming mitigation.

Enteric CH_4 from ruminant livestock is produced and released into the atmosphere through rumen microbial methanogenesis (Morgavi et al., 2010). Methanogenic archaea (methanogens) intercept substrate CO_2 and H_2 liberated during bacterial fermentation of feed materials (Kamra, 2005), and during this inefficient digestion process (Herrero and Thornton, 2013; Patra, 2012), methanogen metabolism leads to reductive CH_4 production and loss of feed energy as CH_4 emissions. To abate enteric methanogenesis, different strategies such as feeding management and antimethanogenic feed ingredients, have been proposed and assessed (e.g., Moate et al., 2016; Mayberry et al., 2019; Beauchemin et al., 2020). Some types of macroalgae have been demonstrated to mitigate production of CH_4 during *in vitro* and *in vivo* rumen fermentation significantly (Machado et al., 2014; Kinley and Fredeen 2015; Li et al., 2018; Kinley et al., 2020; Abbott et al., 2020). Among the different macroalgae species, Kinley et al. (2016a) concluded that the red algae *Asparagopsis* spp. showed the most potential for reducing CH_4 production. Kinley et al. (2016b) further demonstrated that forage with the addition of 2% *Asparagopsis taxiformis* could eliminate CH_4 production *in vitro* without negative effects on forage digestibility. In recent animal experiments, reduction of enteric CH_4 production by more than 98% was achieved with only 0.2% addition of freeze-dried and milled *Asparagopsis taxiformis* to the to the organic matter (OM) content of feedlot cattle feed (Kinley et al., 2020).

Halogenated, biologically active secondary metabolites are pivotal in the reduction of CH_4 induced by Asparagopsis (Abbott et al., 2020). Most of the reduction is ascribed to bromoform ($CHBr_3$) inhibition of the CH_4 biosynthetic pathway within methanogens (Machado et al., 2016). $CHBr_3$ as

a natural halogenated volatile organic compound originates from chemical and biological sources including marine phytoplankton and macroalgae (Carpenter and Liss, 2000; Quack and Wallace, 2003). When emitted to the atmosphere, $CHBr_3$ has an atmospheric lifetime shorter than six months and is often referred to as a very short-lived substance (VSLS). Once released into the atmosphere, degraded halogenated VSLSs can catalytically destroy ozone in the troposphere and stratosphere, thus drawing them considerable interest (Engel and Rigby et al., 2018; Zhang et al., 2020). Bromoform is the dominant compound among bromine-containing VSLSs emissions, resulting mostly from natural sources (Quack and Wallace, 2003) and to a lesser degree from anthropogenic production (Maas et al., 2019; 2021). With an atmospheric lifetime of about 17 days (Carpenter and Reimann et al., 2014), $CHBr_3$ can deliver bromine to the stratosphere under appropriate conditions of emission strength and vertical transport (e.g., Aschmann et al., 2009; Liang et al., 2010; Tegtmeier et al., 2015, 2020) and thus contribute to ozone depletion in the lower and middle stratosphere (e.g., Yang et al., 2014; Sinnhuber and Meul, 2015). Global research on enabling large-scale seaweed *Asparagopsis* farming is increasing (Black et al., 2021) as it appears to be one of the most promising options as an antimethanogenic feed ingredient to achieve carbon neutrality in the livestock sector within the next decade (Kinley et al., 2020; Roque et al., 2021). In consequence, the environmental impact of $CHBr_3$ due to *Asparagopsis* farming also needs to be explored and elucidated. In this study, only the impact on the stratosphere is considered.

The hypothesis was that large scale cultivation of *Asparagopsis* would not contribute significantly to depletion of the ozone layer. The aim of this study was to assess the impact of anthropogenic and natural processes that may contribute to $CHBr_3$ emissions inherent in large scale production of *Asparagopisis spp.* and the subsequent impact of $CHBr_3$ release to the atmosphere by using cultivation in Australia as the model. Specific objectives were to inform the industry, policy makers, as well as the scientific community on: (i) the potential impact of $CHBr_3$ associated with mass production of *Asparagopsis* on atmospheric halogen budgets and ozone depletion; (ii) potential impacts relative to variability in regional climate, atmospheric conditions, and convection trends with different potentials for transport of $CHBr_3$ to stratospheric ozone; (iii) the combined $CHBr_3$ emissions potential of ocean and terrestrial based cultivation of *Asparagopsis* to supply sufficient biomass for up to 50% of beef feedlot and dairy cattle in Australia; and (iv) extrapolation of the impacts of production to requirements on a global scale.

2. Data and Method

The potential impact of $CHBr_3$ on the atmospheric bromine budget and stratospheric ozone depletion, associated with *Asparagopsis spp.* mass production was assessed for assumed annual yields and particular production scenarios of macroalgae in Australia. Terrestrial systems cultivation and open ocean cultivation under different harvest conditions, variations of seaweed yield and growth rates for various scenarios and locations were tested as described in the following subsections.

2.1 Cultivation Scenarios

The cultivation scenarios in this study assume that sufficient seaweed is grown to supply *Asparagopsis spp.* to 50% of the Australian herds of beef cattle in feedlots (100%: ~1.0×10^6) and dairy cows (100%: ~1.5×10^6). For an effective reduction of CH_4 production from ruminants, a ~0.4% addition of freeze-dried and milled *Asparagopsis taxiformis* to the daily feed dry matter intake (DMI) is required (Kinley et al., 2020). This results in daily feed additions of 38 g dry weight (DW) *Asparagopsis* per head of feedlot cattle and 94 g DW *Asparagopsis* per head of dairy cows. In total, the required annual yield amounts to ~3.5×10^4 Mg DW *Asparagopsis* to supplement the feed of roughly 50% of the Australian feedlot cattle and Australian dairy cows. Assuming that fresh weight (FW) has a DW content of 15%, a total of ~2.3×10^5 Mg FW *Asparagopsis* needs to be harvested every year.

For a global scenario, we make the functional assumptions that: (i) there would be adoption of 30% of the global feed base to be supplemented with *Asparagopsis* farmed in Australia to reduce ruminant CH_4 production worldwide; (ii) *Asparagopsis* would be adopted by 50% of Australia's feedlot and dairy industries; and (iii) this is approximately equivalent to 1% of the global feedlot and dairy herds for the purpose of both assumed magnitude of production and adoption relevant for calculations of supply and emissions. This export scenario requires for 30 times increased production compared to the Australian scenario if all the required *Aspargopsis* was to be cultivated in Australia and an annual harvest of ~1 Tg DW *Asparagopsis* would be needed from Australian waters.

For the future farm distributions in Australia, we assume that *Asparagopsis* will be cultivated in open ocean systems and terrestrial confinement systems (that may include, but not limited to, tanks,

raceways, and ponds) located near Geraldton, Triabunna, and Yamba (Figure 1). We assume that one third of the required annual yield (~1.2×10^4 Mg DW) is grown near Triabunna (T), with 60% in terrestrial systems and 40% in open ocean farms, one third is grown in terrestrial systems at Yamba (Y), and the last third is grown in the open ocean in Geraldton (G). For comparison of the environmental impact, we also adopt a tropical scenario where all farms with their total annual yield of ~3.5×10^4 Mg DW are assumed to be situated near Darwin.

The emissions of $CHBr_3$ from the macroalgae farms can be derived based on estimates of the standing stock biomass. For any given farming scenario, the standing stock biomass B_f (g DW) is a function of time t and can be calculated from the initial biomass B_i (g DW) and the specific growth rate GR (%/day) according to Hung et al. (2009):

$$B_f(t) = B_i \cdot (1 + GR/100)^t \quad (1)$$

Terrestrial systems and open ocean cultivation scenarios are assuming a fixed targeted annual yield. For a given initial biomass and growth rate, the length and frequency of the growth periods per year need to be chosen accordingly, to achieve the required final yield. Yong et al. (2013) checked the reliability of different equations for seaweed growth rate determination by comparing the daily seaweed weight cultivated under optimized growth condition, and the most reliable relationship between initial and final weight leads to the form of Eq (1). We also applied several growth rates from 1 to 10% to show the possible influence of this parameter on the overall emissions of the algae. Average growth rates of *Asparagopsis* ranged from 7 to 13 %/day in samples from tropical and sub-tropical Australia during short-term experiments (Mata et al., 2017). We used a lower growth rate of 5% for our scenario to provide an upper estimate of potential $CHBr_3$ emissions. Note that emissions decrease by 27% when using a growth rate of 7% as demonstrated in section 3.1.

Figure 2 provides an example of the variations of standing stock of *Asparagopsis* for the farms of Geraldton (all open ocean) and Yamba (all terrestrial systems) with a growth rate of 5% per day. For the open ocean cultures, we assume a scenario of six harvests per year and 60 day growth periods to obtain the annual yield (Battaglia, 2020; Elsom, 2020). For a sensitivity study, we assume an alternative scenario based on the same initial biomass, but only one harvest per year. As evident from Figure 2, the same annual yield can be achieved with one harvest per year if

applying an extended growth period of 96 days. For the tank cultures, a harvest every 5 days (73 harvests per year) is assumed as a realistic scenario (Battaglia, 2020; Elsom, 2020).

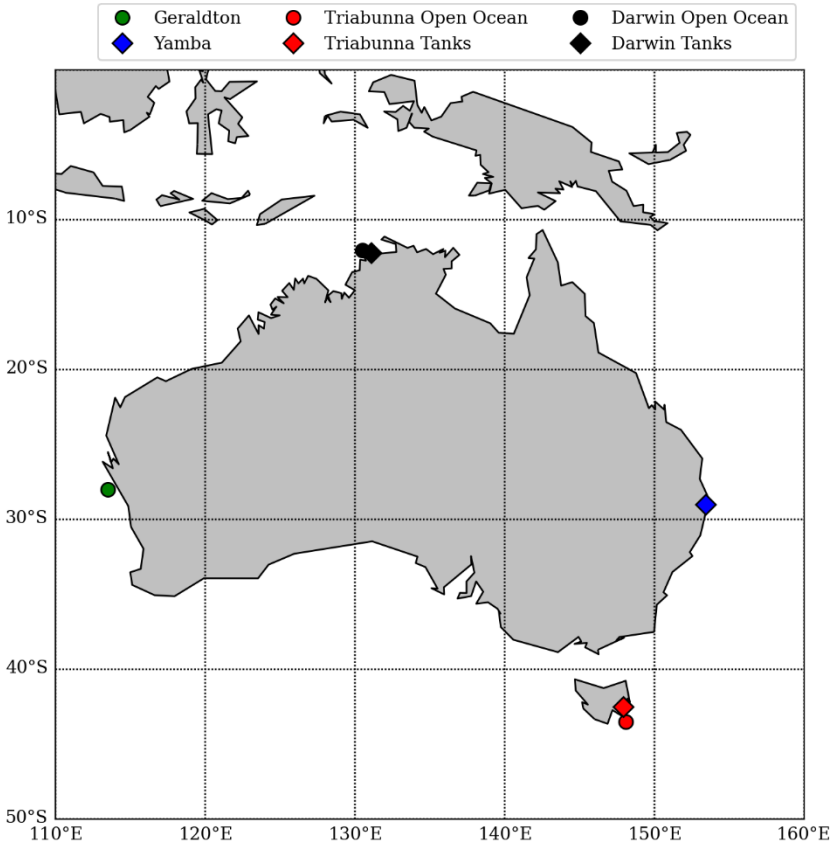

Figure 1. Locations of actual *Asparagopsis* farms in Geraldton, Triabunna, Yamba, and theoretical farms in Darwin.

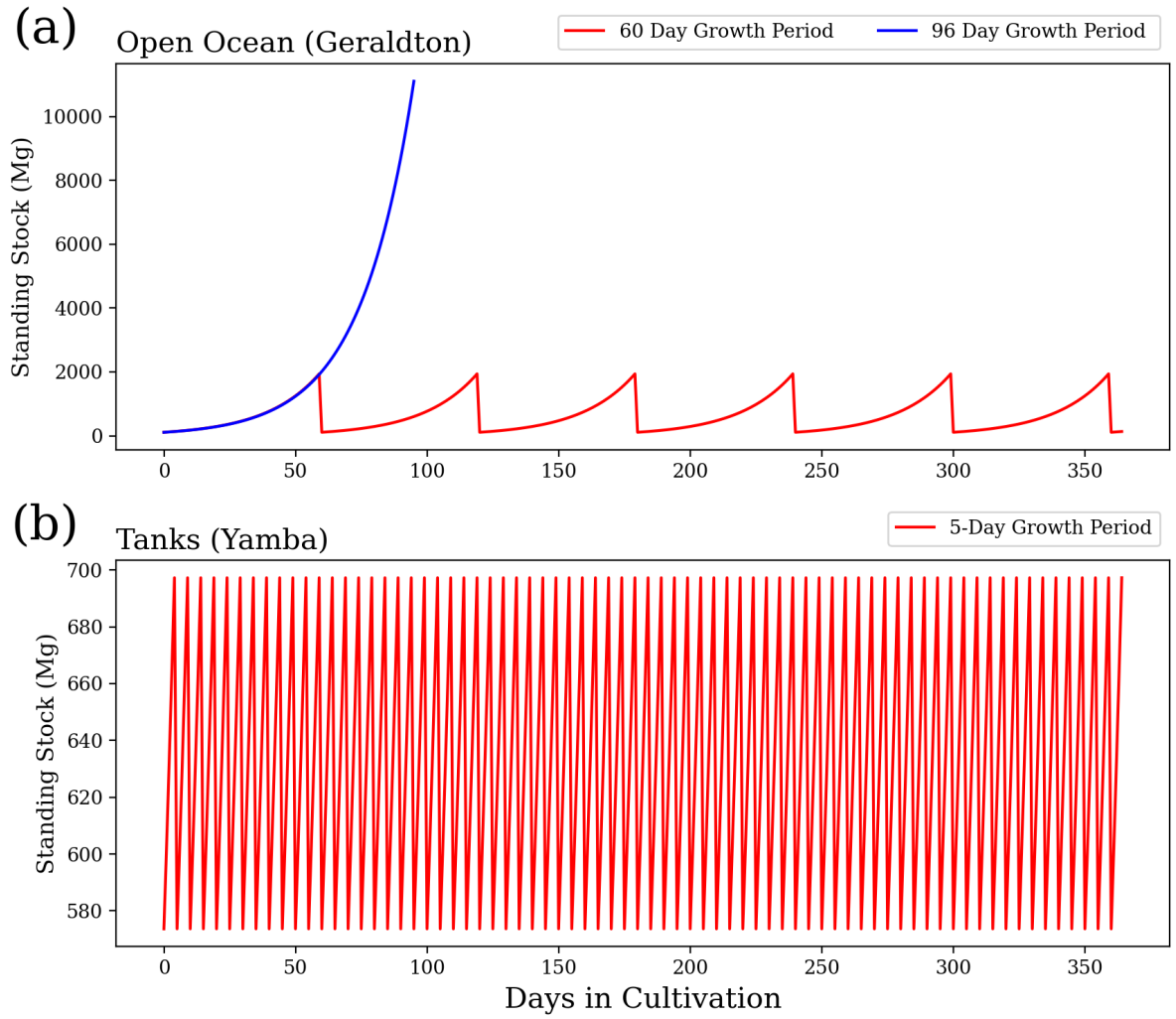

Figure 2. Standing stock biomass of *Asparagopsis* cultivation a) in the open ocean for a 60-day growth period and 96 day growth period and b) in terrestrial systems culture for a 5 day growth period. Each of the three scenarios will achieve an annual yield of ~1.6×10^4 Mg DW.

2.2 *Asparagopsis* $CHBr_3$ release rates

Rates of the $CHBr_3$ content in *Asparagopsis* given in the literature range between 3.4 to 43 mg $CHBr_3$/g DW, with values around 10 mg $CHBr_3$/g DW appearing to be realistic in current cultivation (Burreson and Moore, 1976; Mata et al., 2012, 2017; Paul et al., 2006; Vucko et al., 2017). We assume that *Asparagopsis* strain selection cultivated for feed supplements will lead to high yielding $CHBr_3$ varieties thus we assume augmented $CHBr_3$ production with a mean content

of 21.7 mg $CHBr_3$/g DW (Magnusson et al., 2020) for this study.

Very few values on the $CHBr_3$ release from *Asparagopsis* have been reported in the literature. A constant release of 1100 ng $CHBr_3$/g DW hr^{-1} was measured for *Asparagopsis armata tetrasporophyte*, which has a $CHBr_3$ content of 14.5 mg $CHBr_3$/g DW (Paul et al., 2006). We assume a linear scaling between the $CHBr_3$ release rates and the content. Thus, a cultivated *Asparagopsis* for which we assume 21.7 mg $CHBr_3$/g DW should release around 1646 ng $CHBr_3$/g DW hr^{-1}, a rate which has been confirmed by Marshall et al. (1999). Therefore, for our calculations, we assume a constant release of 1600 ng $CHBr_3$/g DW hr^{-1} for farmed *Asparagopsis* with a $CHBr_3$ content of 21.7 mg $CHBr_3$/g DW. These content and release rates are higher than those for wild stock algae (Leedham et al., 2013; Nightingale et al., 1995) as the farming aims at algae varieties with high $CHBr_3$ yield. As available information on this topic is very sparse no variations of the release rate with life-cycle stages, season, location, or other environmental parameters were used in this study. Also, the two species *Asparagopsis armata* and *Asparagopsis taxiformis* were treated the same way as *Asparagopsis spp*., as variations in $CHBr_3$ content and release within or between species are currently unknown (Mata et al., 2017) and more research on this topic is needed.

2.3 Parameterization of $CHBr_3$ Emission

The emissions of $CHBr_3$ from farmed macroalgae are a function of the standing stock biomass (in g DW) and can be calculated with the constant release rate (R_{CHBr_3}) of 1600 ng $CHBr_3$/g DW hr^{-1} multiplied with the standing stock. The total release of $CHBr_3$ (E_{CHBr_3}) over the complete growth period of T days is given by the integral over the daily emissions from day 1 to day *T*:

$$E_{CHBr_3} = \int_0^T 24 \cdot B_i \cdot (1+GR)^t \cdot R_{CHBr_3} dt = 24 \cdot B_i \cdot R_{CHBr_3} \cdot \frac{[(1+GR)^T - 1]}{ln\,(1+GR)} \qquad (2)$$

For our atmospheric impact studies we assume, that all $CHBr_3$ released from the algae is emitted into the atmosphere at its location of production. An increasing seawater concentration of $CHBr_3$ shifts the equilibrium conditions between seawater and air towards the atmosphere, as $CHBr_3$ easily volatilizes to the atmosphere. Consequently, air-sea exchange acts as a relatively fast loss process for $CHBr_3$ in surface water. Oceanic sinks can also impact $CHBr_3$, but act on relatively long timescales. Degradation through halide substitution and hydrolysis results in the ocean sink $CHBr_3$ half-life of 4.37 years (Hense and Quack, 2009). Thus, most of the $CHBr_3$ contained in

surface seawater is instantly outgassed into the atmosphere without oceanic loss processes, playing a role as confirmed by the modelling study of Maas et al. (2021).

The air-sea exchange of $CHBr_3$ is expressed as the product of its transfer coefficient (k_w) and the concentration gradient (Δc) (Eq. (3)). The gradient is computed between the water concentration (c_w) and theoretical equilibrium water concentration (c_{atm}/H), where c_{atm} is the atmospheric concentration and H is Henry's law constant (Moore et al., 1995a; Moore et al., 1995b).

$$F = k_w \cdot \Delta c = k_w \cdot (c_w - \frac{c_{atm}}{H}) \quad (3)$$

The compound-specific transfer coefficient (kw) is determined using the air-sea gas exchange parameterization of Nightingale et al. (2000) (Eq. (4))

$$k_w = k \cdot \sqrt{Sc}/660 \quad (4)$$

The transfer coefficient k is a function of the wind speed at 10 m height (u_{10}): $k = 0.2u_{10}^2 + 0.3u_{10}$, and the Schmidt number (Sc) is a function of sea surface temperature (SST) from Quack and Wallace (2003), which is expressed as $Sc = 4662.8 - 319.45 \cdot SST + 9.9012 \cdot SST^2 + 0.1159 \cdot SST^3$.

In this study, we use the $CHBr_3$ sea-to-air flux climatology from Ziska et al. (2013) as marine background emissions. The global emission scenario from Ziska et al. (2013) is a bottom-up estimate of the oceanic $CHBr_3$ fluxes, generated from atmospheric and oceanic surface ship-borne *in situ* measurements between 1979 to 2013. Due to the paucity of data, the 35 year mean gridded data set was filled by interpolating and extrapolating the *in situ* measurement data. The oceanic emissions were calculated with the transfer coefficient parameterization of Nightingale et al. (2000) and 6-hourly meteorological data, which allow a temporal emission variability related to wind and temperature.

2.4 Emission Scenarios for FLEXPART Simulations

To quantify the atmospheric impact of $CHBr_3$ emissions from macroalgae farming, the Lagrangian particle dispersion model FLEXPART (Pisso et al., 2019) is used. FLEXPART has been evaluated extensively in previous studies (e.g., Stohl et al., 1998; Stohl and Trickl, 1999). The model includes moist convection and turbulence parameterizations in the atmospheric boundary layer and free troposphere (Forster et al., 2007; Stohl and Thomson, 1999). The European Centre for Medium-Range Weather Forecasts (ECMWF) reanalysis product ERA-Interim (Dee et al., 2011) with a

horizontal resolution of 1° x 1° and 60 vertical model levels is used for the meteorological input fields, providing air temperature, winds, boundary layer height, specific humidity, as well as convective and large-scale precipitation with a 3-hour temporal resolution.

We conduct FLEXPART simulations for year 2018 with different emission scenarios as explained in the following and summarized in Table 1:

1.) Australian scenarios: $CHBr_3$ emissions from the *Asparagopsis* farming in Geraldton, Triabunna, and Yamba are calculated for an overall annual yield of 34674 Mg DW according to Equation 2. For the terrestrial systems, 5 day growth periods are assumed resulting in 73 harvests per year. For the open ocean, the assumption of different growth periods results in three sub-scenarios a) 6 times 60 day growth periods with the first period starting on January 1st (referred to as GTY_O60), b) one 96 day growth period starting on January 1st (GTY_O96_Jan), and c) and another starting on July 1st (GTY_O96_Jul).

For the last Australian scenario, we assume that all farms are located around Darwin in the Northern Territory tropics with 6 times 60 day growth periods in the open ocean and 73 times 5 day growth periods in the terrestrial systems (Darwin_O60). While this is an unlikely scenario according to current plans, it is useful to demonstrate the influence of potential farming locations on their environmental impact.

2.) Global scenarios: Emissions from *Asparagopsis* farming in Geraldton, Triabunna, and Yamba are estimated according to the annual yield, upscaled by a factor of 30 to global requirements. amounting to 1.04×10^6 Mg DW. Growth periods and harvesting frequencies are set up in the same way as for the Australian scenarios. Short names of the global scenarios are the same as for the Australian scenarios with the additional label 30x.

3) Background scenario: Emission from Ziska et al. (2013) for the entire coastal region around Australia defined as all 1°x1° grid cells directly neighbouring the coastline (Ziska_Coast).

4.) Extreme event scenarios: We assume extreme conditions where a hypothetical tropical cyclone causes implausible release of all $CHBr_3$ from the macroalgae farm and water into the atmosphere. We focus on the case study of Geraldton and the tropical cyclone Joyce, which occurred from 6-13 January 2018 around western Australia. We base the amount of available macroalgae biomass on the Australian scenario and assume that the entire $CHBr_3$ content of all *Asparagopsis* at this location is released at once. The two scenarios defined here assume that the tropical cyclone occurs at the end of the 60 day growth period (Geraldton_Ex60) resulting in the release of 41.8 Mg $CHBr_3$

(21.7 mg $CHBr_3$/g DW * 1926 Mg DW) or at the end of the 96 day growth period (Geraldton_Ex96) resulting in the release of 250.8 Mg $CHBr_3$ (21.7 mg $CHBr_3$ /g DW* 11558 Mg DW).

The daily model output is recorded for all simulations. For the extreme event, which assumes the destruction of a farm (Geraldton-Ex), the 3 hourly output is recorded. For all simulations, except the background scenario and extreme scenario, trajectories are released from four regions of the size of: a) Geraldton (open ocean, 11558 ha): 0.1°x0.1°; b) Triabunna (open ocean, 4623 ha): 0.06°x0.06°; c) Triabunna (terrestrial systems, 126 ha): 0.01°x0.01°; and d) Yamba (terrestrial systems, 210 ha): 0.01°x0.01°. For the tropical and extreme scenarios, trajectories are released from the Darwin and Geraldton farms, respectively. For the background scenario Ziska_Coast, trajectories are released from the 1.0°x1.0° grid along the Australian coastline. Note that it is not reasonable to compute the Ziska emission on the locations of farming as some farms are terrestrial. However, if we assume all the farms are Geraldton-like (i.e., all grown in the open ocean), the Ziska emission in Geraldton, Yamba and Triabunna will be 843 Mg, 295 Mg, and 676 Mg, respectively. The amount of released $CHBr_3$ is evenly distributed among the trajectories and is depleted during the Lagrangian simulations according to the atmospheric half-life of 17 days (*e*-folding lifetime of 24 days) (Hossaini et al., 2010; Montzka and Reimann et al., 2010; Engel and Rigby et al., 2018).

297 **Table 1.** Detailed information on the scenarios set up for the atmospheric transport simulations
298 with FLEXPART (Geraldton, Triubanna, and Yamba: GTY)

Name		Total Yield (Mg DW)	$CHBr_3$ Emissions (Mg)	Notes	Simulation Period
Australian Scenarios	GTY_O60	Total: 34674 Open Ocean: G: 11558 T: 4623 Y: - Terrestrial systems: G: - T: 6935 Y: 11558	Total: 27.3 Open Ocean: G: 9.10 T: 3.64 Terrestrial systems: T: 5.46 Y: 9.10	6 harvests (every 60 days) in the open ocean; 73 harvests (every 5 days) in the terrestrial systems.	01.01.2018 - 31.12.2018 2-month spin-up
	GTY_O96_Jan			1 harvest (after 96 days) in open ocean; 73 harvests (every 5 days) in terrestrial systems. Growth in open ocean starts from 01.01.2018.	
	GTY_O96_Jul			Same as GTY_O96_Jan but with growth in open ocean starting from 01.07.2018.	
	Darwin_O60	Total: 34674 Open Ocean: Darwin: 16181 Terrestrial systems: Darwin:18493	Total: 27.3 Open Ocean: Darwin: 12.7 Terrestrial systems: Darwin: 14.6	Same as GTY_O60 but with farms near Darwin	
Global Scenarios	GTY_O60_30x	Total: 1040220 Open Ocean G: 346740 T: 138690 Y: - Terrestrial systems: G: - T: 208050 Y: 346740	Total: 819 Open Ocean G: 273 T: 109.2 Terrestrial systems: T: 163.8 Y: 273	Same as GTY_O60 but with initial biomass and areas 30 times larger.	
	GTY_O96_Jan_30x			Same as GTY_O96_Jan but with initial biomass and areas 30 times larger.	
	GTY_O96_Jul_30x			Same as GTY_O96_Jul but with initial biomass and areas 30 times larger.	
	Darwin_O60_30x	Total: 1040220 Open Ocean Darwin: 485430	Total: 819 Open Ocean Darwin: 381 Terrestrial systems: Darwin: 438	Same as Darwin_O60 but with initial biomass and areas 30 times larger.	

		Terrestrial systems: Darwin: 554790			
Background Scenario	Ziska_Coast	-	3109	$CHBr_3$ emission of the coastal region of Australia from Ziska et al. (2013)	
Extreme Scenarios	Geraldton_Ex60	Open Ocean: G: 1926	Open Ocean: G: 41.8	Extreme event: $CHBr_3$ in Geraldton surface water before harvest is released due to tropical cyclone Joyce (07.01.2018 – 15.01.2018). Harvest period: 60 days.	9.01.2018 – 9.02.2018 No spin-up
	Geraldton_Ex96	Open Ocean: G: 11558	Open Ocean: G: 250.8	Same as Geraldton _Ex60 but with harvest period of 96 days	

299
300
301 **2.5 Ozone Depletion Potential (ODP)**
302
303 The ozone depletion potential (ODP) is defined as the time-integrated potential destructive effect
304 of a substance to the ozone layer relative to that of the reference substance CFC-11 (CCl_3F) on a
305 mass emitted basis (Wuebbles, 1983). The ODP is a well-established and extensively used concept
306 traditionally defined for anthropogenic long-lived halocarbons. However, the concept has been
307 also applied to VSLSs (Brioude et al., 2010; Pisso et al., 2010): unlike the ODP for long-lived
308 halocarbons, which is one constant number, the ODP of a VSLS is a function of time and location
309 of the emissions. This variable number still describes the time-integrated ozone depletion resulting
310 from a $CHBr_3$ unit mass emission relative to the ozone depletion resulting from the same unit mass
311 emission of CFC-11. The ODP for VSLSs can be derived from chemistry-climate or chemistry
312 transport models simulating the changes of ozone due to certain compound (Claxton et al., 2019;
313 Zhang et al., 2020). The trajectory-derived ODP of VSLSs such as $CHBr_3$ is calculated as a
314 function of location and time of the potential emissions (Brioude et al., 2010; Pisso et al., 2010).
315 As for the traditional ODP concept, the time and space dependent ODP describes only the potential
316 of a compound but not its actual damaging effect to the ozone layer and is independent of the total
317 emissions. It is noteworthy that many VSLSs including $CHBr_3$ can impact ozone in the troposphere
318 and stratosphere. As ODPs are used to assess stratospheric ozone depletion only, the contribution
319 of VSLSs to tropospheric ozone destruction needs to be excluded when calculating their ODP
320 (Pisso et al., 2010; Zhang et al., 2020). The trajectory based ODP from Pisso et al. (2010) used in
321 this study considers only the impact of $CHBr_3$ on the stratospheric ozone instead of the ozone

column. The fraction of originally emitted VSLSs reaching the stratosphere depends strongly on the meteorological conditions. In particular, it shows a pronounced seasonality. Here we apply ODP values adapted from Pisso et al. (2010), originally calculated for a VSLS with a lifetime of 20 days, which is very similar to that of $CHBr_3$. ODPs for VSLSs are calculated by means of combining two sources of information: one corresponding to the slow stratospheric branch and the other to the fast tropospheric branch of transport. The former is uniform for all species modelled and is based on the calculation of the expected stratospheric residence time of a Lagrangian particle entering the stratosphere. The latter is based on the probability of stratospheric injection of a given unit emission of the tracer at the ground. The probability of injection depends not only on the fraction of air reaching the tropopause but also on the time the air mass takes from the ground to the tropopause. This is because during the transit of the air mass through the troposphere, the precursor is chemically degraded, and the solubility of the products leads to mass loss due to wet deposition.

In this study, we present the ODP-weighted emissions, which combine the information of the ODP and surface emissions and are calculated by multiplying the $CHBr_3$ emissions with the trajectory-derived ODP at each grid point. The ODP-weighted emissions provide insight into key factors of $CHBr_3$ emission (i.e., where and when $CHBr_3$ is emitted) that impact stratospheric ozone (Tegtmeier et al., 2015). The absolute values are subject to relatively large uncertainties arising from uncertainties in the parameterization of the convective transport. Furthermore, the ODP values applied here do not consider product gas entrainment and provide therefore a lower limit of the impact of $CHBr_3$ on stratospheric ozone. Taking into account product gas entrainment can lead to 30% higher ODP values (Engel and Rigby et al., 2018; Tegtmeier et al., 2020), but has no large impact on the comparison between global ODP-weighted $CHBr_3$ emissions and farm-based ODP-weighted $CHBr_3$ emissions presented here.

3. $CHBr_3$ Emission and Atmospheric Mixing Ratio

3.1 $CHBr_3$ Emissions

As shown in Eq. (2), the total $CHBr_3$ emissions are determined by the growth rate, growth period and initial biomass. For our scenarios based on selected fixed growth rates, the growth periods are adjusted so that the intended annual yield (~3.5×10^4 Mg DW) is achieved. We conduct a sensitivity

study to analyze how much the total emissions change for variations of the length and number of the growth periods for a fixed annual yield. For this purpose, we compare Geraldton farming for GTY_O60 (open ocean, six 60 day growth periods) with Geraldton farming for GTY_O96 (open ocean, one 96 day growth period) and Yamba farming for GTY_O60 (terrestrial systems, 73 growth periods of 5 days). Our estimates show that the annual release of $CHBr_3$ from Asparagopsis is the same for all three case studies (Fig. 3a), confirming that for a fixed annual yield and growth rate, the culture conditions of open ocean and tank farming are not important for VSLSs emissions. A second sensitivity study investigates the variations of $CHBr_3$ emissions for different growth rates and the same fixed annual yield. For this purpose, we compare Geraldton farming (open ocean, with an intended annual yield of ~1.1×10^4 Mg DW) for different growth rates varying between 1% and 10%. The scenario with a 5% growth rate corresponds to Geraldton farming for GTY_O60 (open ocean, six 60 day growth periods), while for the other growth rates the growth periods have been adjusted to achieve the same annual yield.

The $CHBr_3$ emissions depend strongly on the growth rates (Fig 3b), with emission calculated for a 1% growth rate being almost 10 times higher than the emissions calculated for a 10% growth rate. For a lower growth rate, the initial biomass needs to be higher to achieve the targeted seaweed yield (~1.1×10^4 Mg) after one year and/or the growth period needs to be longer, thus resulting in larger amounts of biomass in the ocean and higher annual $CHBr_3$ emissions. Vice versa, for higher growth rates, the annual oceanic biomass is smaller and total emissions are lower.

The overall emissions from the intended Australian seaweed farming of ~3.5×10^4 Mg DW range from 13.5 Mg (0.05 Mmol) for a 10% growth rate to 134 Mg (0.5 Mmol) per year for a 1% growth rate. For the growth rates higher than 5%, the differences of $CHBr_3$ emissions are less significant than those derived for the lower growth rates. In our study, we choose 5% growth rate as representative, which leads to emissions of ~27 Mg (0.1 Mmol) $CHBr_3$ per year for the targeted final yield. For the global scenario with an annual yield of ~1.0×10^6 Mg DW (30 times of the Australian target), the emissions would range from 412 Mg (1.6 Mmol) to 4014 Mg (16 Mmol) per year, with the annual emission of 810 Mg (3.2 Mmol) for 5% growth rates.

Interestingly, the potential local emissions for all the farming scenarios are generally 3 to 6 orders of magnitude higher than the background coastal emissions. The maximum climatological emissions derived from available observations (Ziska_Coast) are around 2000 pmol m^{-2} hr^{-1} for the coastal waters of Australia, while the emissions from an *Asparagopsis* farm can reach more

than 2.0×10^6 pmol (2 µmol) m^{-2} hr^{-1} from a terrestrial system and more than 5.0×10^5 pmol m^{-2} hr^{-1} from the open ocean. These differences are to a large degree related to the fact that the Ziska_Coast is given on a 1.0°x1.0° grid, with high coastal values averaging out over the relatively wide grid cells, while the values derived for the farms apply to much smaller areas. Tank emission rates (0.01°x0.01°) and open ocean farming emission rates (0.1°x0.1°) averaged over a 1°x1° grid cell result in 200 pmol $CHBr_3$ m^{-2} hr^{-1} and 5000 pmol $CHBr_3$ m^{-2} hr^{-1}, respectively, thus being very similar to the Ziska emissions.

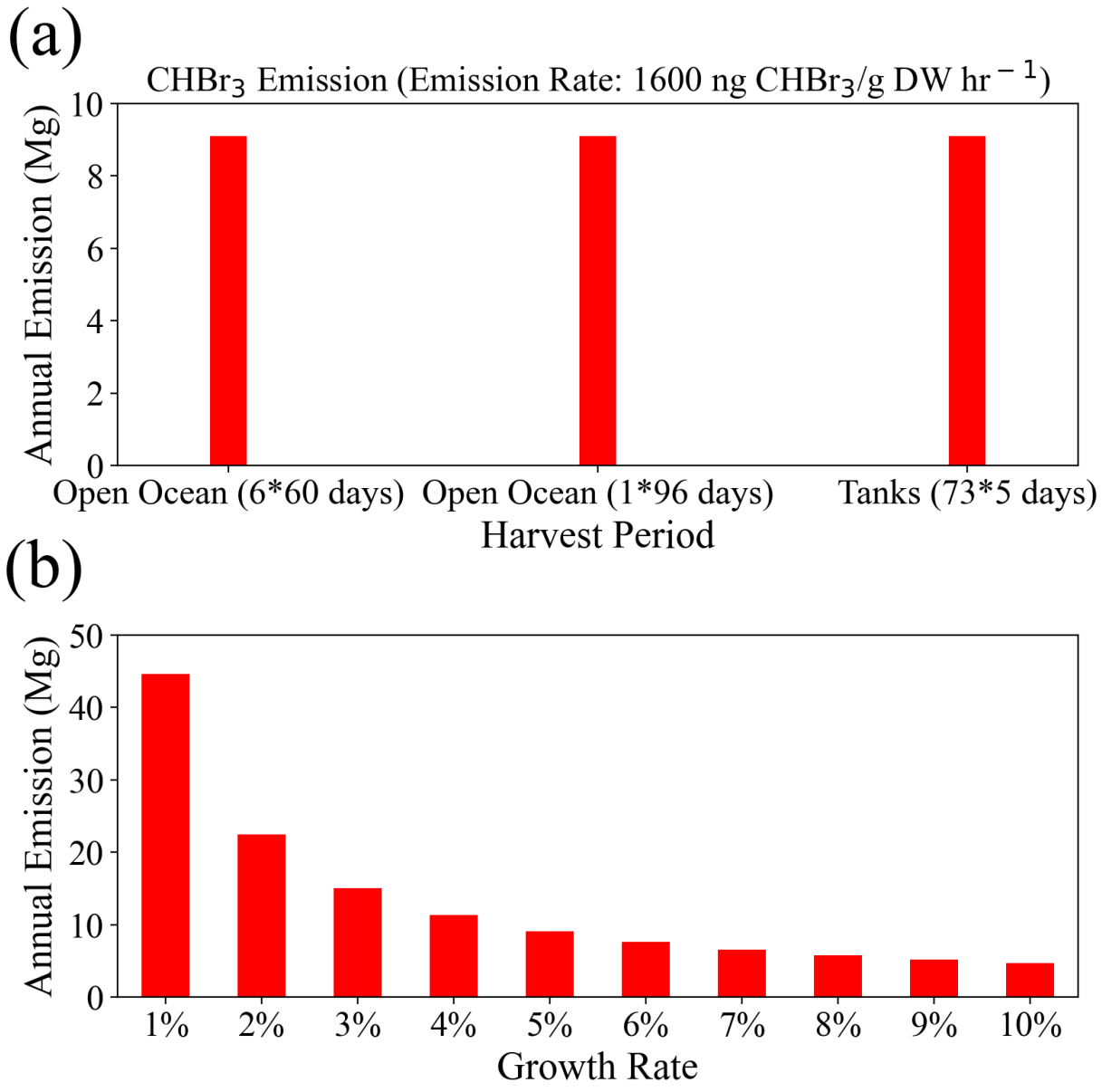

Figure 3. The annual release of $CHBr_3$ (Mg yr^{-1}) from: a) same growth rate (5%) for different growth periods; and b) under different growth rates but with same initial biomass, both a) and b) are obtained with a total annual yield of 11558 Mg DW.

3.2 Atmospheric $CHBr_3$ mixing ratio

We use the $CHBr_3$ emissions calculated in section 3.1 to simulate the enhanced atmospheric $CHBr_3$ mixing ratios (above natural background) for each *Asparagopsis* farming scenario. Background $CHBr_3$ levels are calculated based on the Ziska et al. (2013) Australian coastal emissions (Ziska_Coast). The temporal evolution of $CHBr_3$ mixing ratio with height shows that the $CHBr_3$ resulting from the Australian farming scenarios are negligible (see Figure S1) compared to the coastal background emissions of Australia (Ziska_Coast).

For the global scenarios (Figure 4), atmospheric $CHBr_3$ is comparable to $CHBr_3$ resulting from Australian coastal background emissions, especially near the end of the growth period in the open ocean. For almost all scenarios (except for GTY_O96 _Jul_30x), the emissions generally reach higher into the atmosphere in the first three months of the year with enhanced values around 15 km, reflecting the stronger convection during austral summer. For open ocean emissions occurring during late austral winter (GTY_O96_Jul_30x, Figure 4c), high $CHBr_3$ mixing ratios are found around September, however at a lower altitude range compared to the equivalent scenario with open ocean emission occurring during late austral summer (GTY_O96_Jan_30x; Figure 3b).

The spatial distribution of annual mean $CHBr_3$ at 1 km (Figure 5) further confirms the insignificance of the signals from the Australian farming scenarios compared with the background $CHBr_3$ values. For the global scenarios, localized regions of high mixing ratios are found near the locations of the farms due to the stronger emission. For Darwin_O60_30x, the belt of high mixing ratios is extending northwestward, due to the prevailing easterlies in the tropics. At higher altitudes (e.g., 5 km and 15 km; Figure S2-S3), localized high $CHBr_3$ is only found near Darwin for the Darwin_O60 _30x scenario, reflecting that strong tropical convection is needed to transport short lived gases to such altitudes.

The results above suggest that in the boundary layer, global scenarios and extreme events could lead to $CHBr_3$ comparable mixing ratios as those from the background scenario. Only in the global tropical scenario (Darwin_O60 _30x), $CHBr_3$ mixing ratios, which are larger than the background values, can be found at high altitudes (Figure 4).

Simulations of the two extreme scenarios (Geraldton_Ex) for 60 and 96 day growth periods are shown in Figure 6. For the Geraldton_Ex simulations, we assume the implausible scenario that the farm could be totally damaged by cyclone Joyce on the day of harvest in January and the total $CHBr_3$ content of the *Asparagopsis* stock was simultaneously released to the atmosphere during the event. Both scenarios lead to significant $CHBr_3$ mixing ratios in the atmosphere, especially at altitudes below 5 km. Among the two scenarios, the Geraldton_Ex96 contributes the larger amount of $CHBr_3$ emission, as the macroalgae experienced a longer growth period, so the biomass was higher and had accumulated more $CHBr_3$. When averaged over the same period (Jan 9-Jan 26, 2018), the $CHBr_3$ mixing ratios from Geraldton_Ex96 are much larger than those from Ziska_Coast (Figure 6) below 5 km, and signals with comparable magnitudes, though with smaller coverage, are found at 15 km.

As mentioned in section 3.1, the local $CHBr_3$ emissions due to the seaweed cultivation are generally higher than coastal emission given on 1.0x1.0 grid. However, due to the relatively small spatial extent of the farms, the emissions quickly dilute in the atmosphere, and the magnitude of the mixing ratios decline rapidly off the coast and vertically.

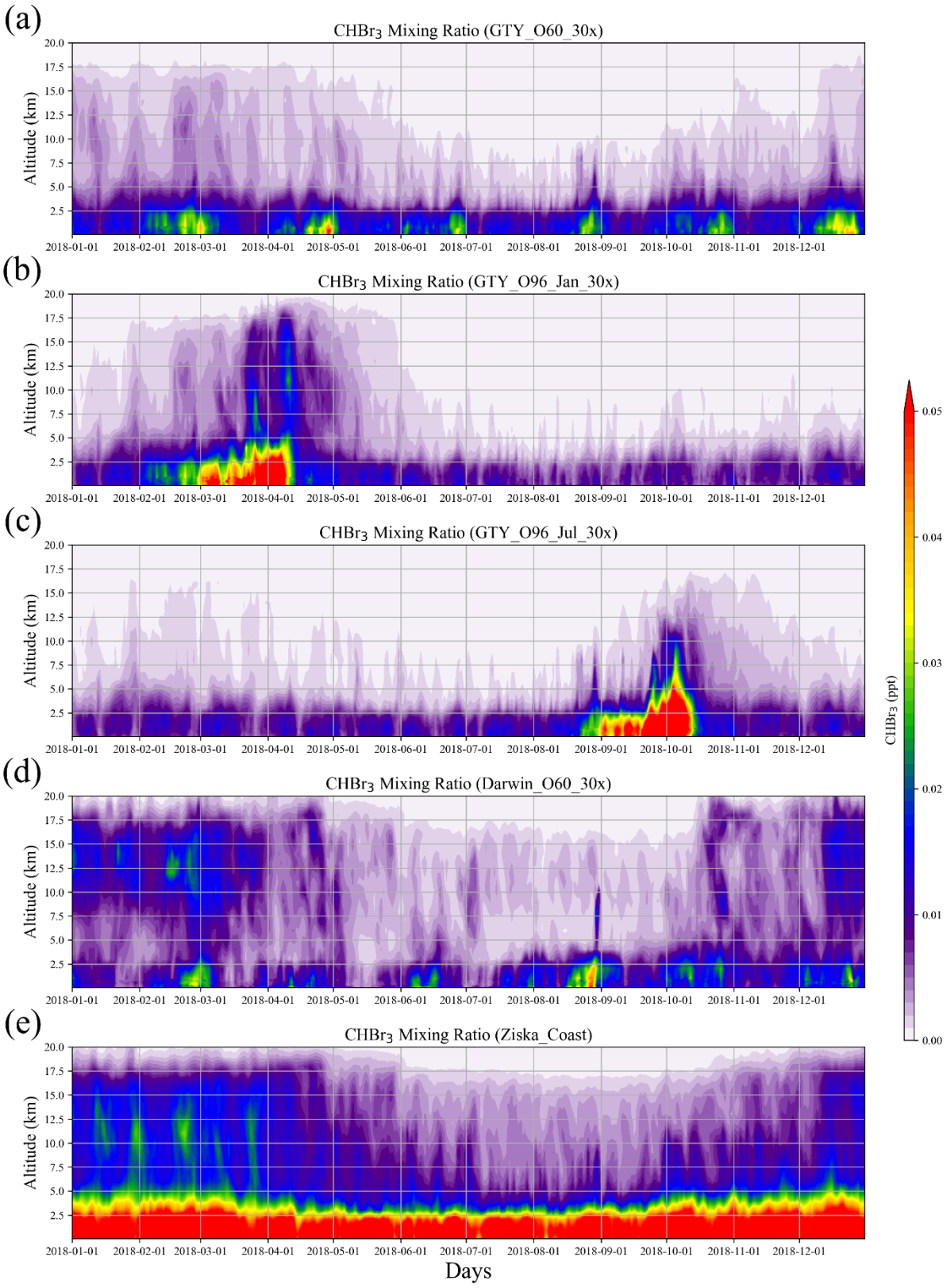
(a)
CHBr3 Mixing Ratio (GTY_O60_30x)
(b)
CHBr3 Mixing Ratio (GTY_O96_Jan_30x)
(c)
CHBr3 Mixing Ratio (GTY_O96_Jul_30x)
(d)
CHBr3 Mixing Ratio (Darwin_O60_30x)
(e)
CHBr3 Mixing Ratio (Ziska_Coast)
Altitude (km)
20.0
17.5
15.0
12.5
10.0
7.5
5.0
2.5
2018-01-01
2018-02-01
2018-03-01
2018-04-01
2018-05-01
2018-06-01
2018-07-01
2018-08-01
2018-09-01
2018-10-01
2018-11-01
2018-12-01
Days
CHBr3 (ppt)
0.05
0.04
0.03
0.02
0.01
0.00

444

Figure 4. Altitude-time cross-sections of $CHBr_3$ mixing ratio averaged over [10°-45° S, 105°-165° E] from Global Scenarios: a) GTY_O60_30x, b) GTY_O96_Jan_30x, c) GTY_O96_Jul_30x, d) Darwin_O60 _30x, and Background Scenario: e) Ziska_Coast.

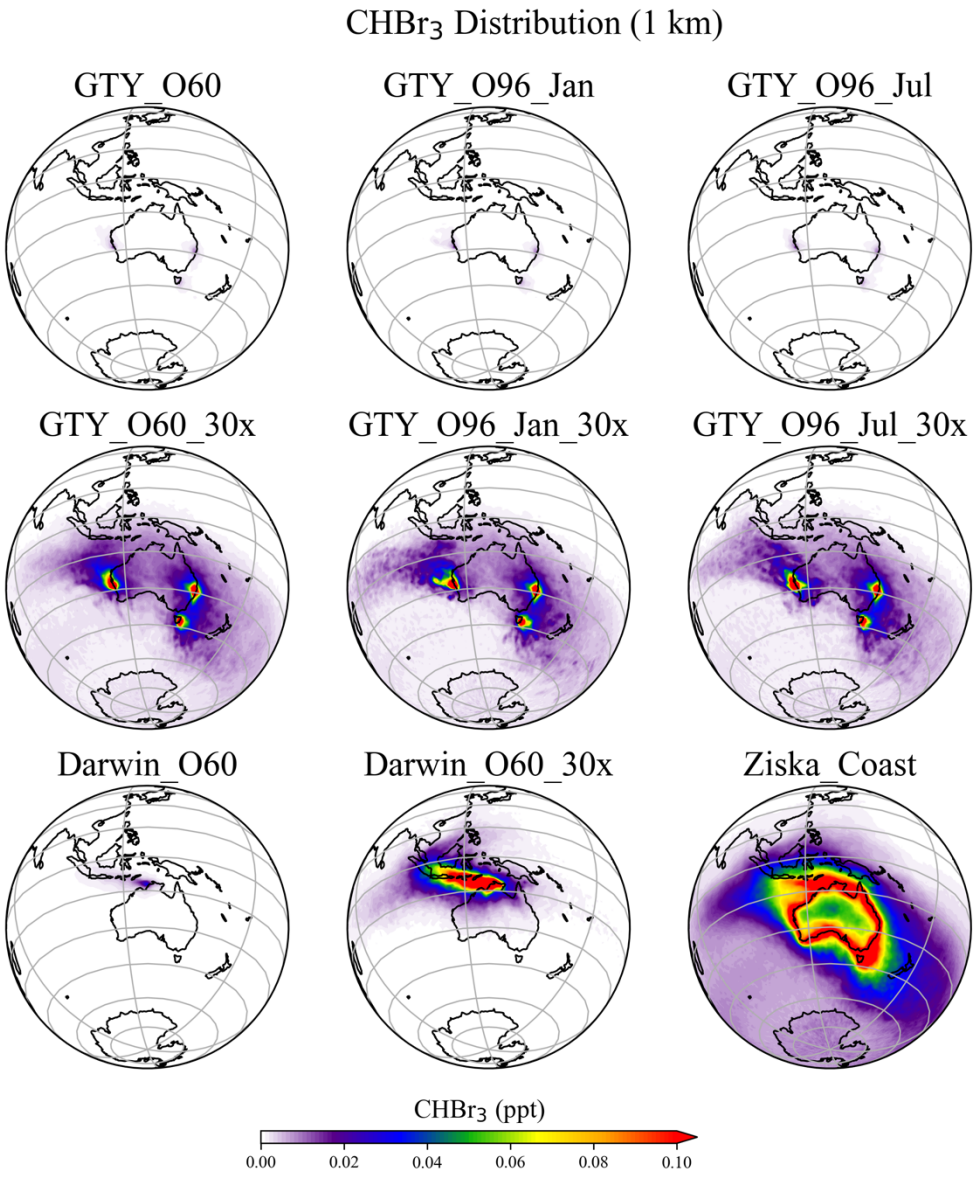

Figure 5. Annual mean $CHBr_3$ spatial distribution from GTY_O60, GTY_O60_30x, GTY_O96_Jan, GTY_O96_Jan_30x, GTY_O96_Jul, GTY_O96_Jul_30x, Darwin_O60, Darwin_O60_30x, and Ziska_Coast at 1 km altitude.

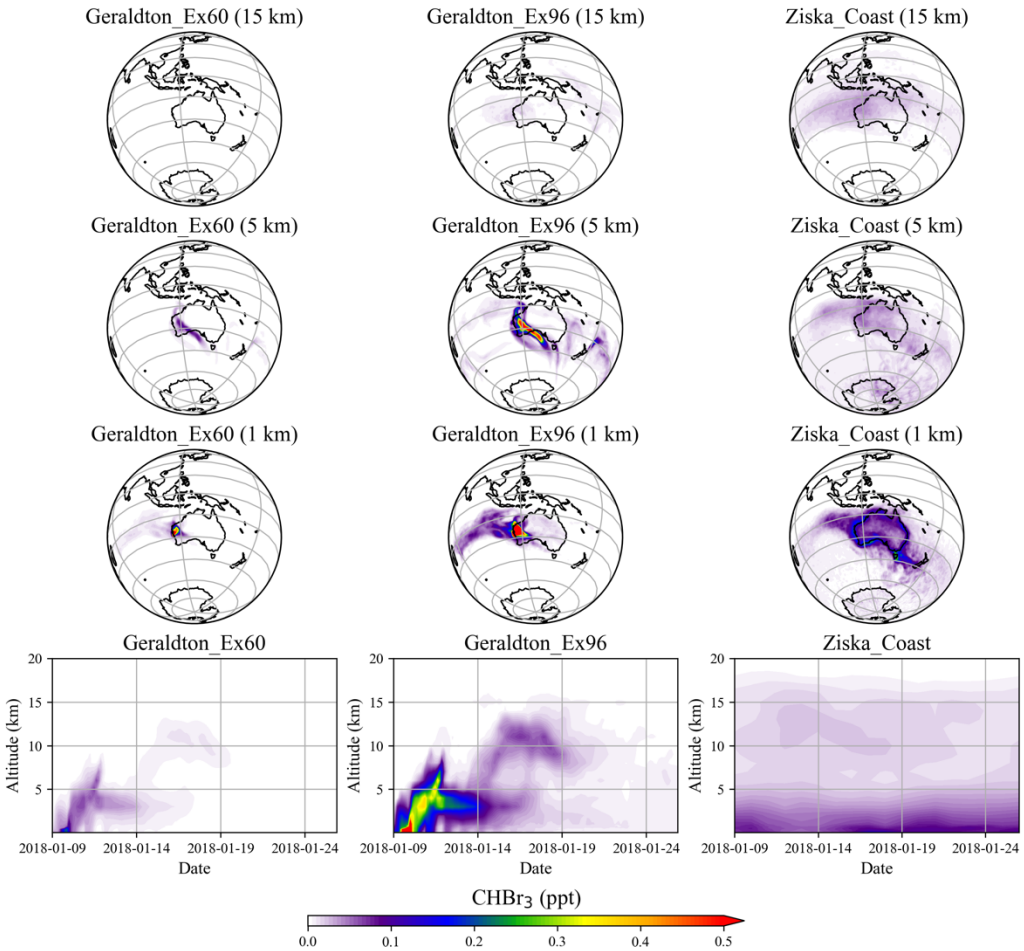

Figure 6. 17-day average of spatial distribution and altitude-time cross-sections of $CHBr_3$ mixing ratio averaged over [10°-45° S, 105°-165° E] for Geraldton_Ex60, Geraldton_Ex96, and Ziska_Coast.

4. Ozone depletion potential for $CHBr_3$

The ODP distribution from Pisso et al. (2010) for the region around Australia, South-East Asia, and the Indian Ocean for the Southern Hemisphere (SH) summer and winter is shown in Figure 7. The ODP distribution changes strongly with season as the transport of short-lived halogenated substances such as $CHBr_3$ depends on the seasonal variations of the location of the Intertropical Convergence Zone (ITCZ). Highest ODP values of 0.5, which imply that any amount (per mass) of $CHBr_3$ released from the specific location will destroy half as much stratospheric ozone as the same amount of CFC-11 released from this location, are found during July over the Maritime continent and during January over the West Pacific south of the equator. The northern Australian

coastline shows highest ODP values during January when the thermal equator and the ITCZ are shifted southwards and ODP values for Yamba and Darwin are 0.26 and 0.29, respectively. The other two locations as well as all four locations during SH winter, show ODP values of only up to 0.1.

As demonstrated in section 3, the total annual $CHBr_3$ emissions from any location are independent of the details of the farming practice, however, the ODP-weighted emissions change for the different scenarios as the growth periods fall into different seasons with varying ODP values. In general, the scenario of one harvest period in SH summer leads to larger ODP-weighted emissions when compared to the same biomass harvested throughout the year. In addition to the harvesting practice, the locations of the farms have a large impact on the efficiency of the $CHBr_3$ transport to the stratosphere and thus on the ODP-weighted emissions.

The ODP-weighted emissions of $CHBr_3$ for different emission scenarios are shown in Figure 8. *Asparagopsis* farming at GTY (GTY_O60) leads to additional $CHBr_3$ emissions of up to 2.53 Mg per year. If all farming (~3.5×10^4 Mg DW *Asparagopsis*) occurs in Darwin (Darwin_O60), ODP-weighted emissions would increase to 6.48 Mg $CHBr_3$ per year. In comparison, all naturally occurring emissions around the Australian coastline (Ziska_coast) lead to OPD-weighted $CHBr_3$ emissions of 221.52 Mg per year. In consequence, *Asparagopsis* farming in the three locations Geraldton, Triabunna and Yamba would lead to an increase of the ODP-weighted emissions from Australian coastal emissions of 1.14%. If all farming would take place in Darwin, ODP-weighted $CHBr_3$ emissions would increase by 2.93%.

As the global ODP-weighted emissions were estimated to be around 4.0×10^4 Mg per year (bottom-most bar in Figure 8., Tegtmeier et al., 2015), the additional contribution due to the Australian farming scenarios in GTY or Darwin would be negligible increasing the contribution of $CHBr_3$ emissions to ozone depletion by 0.006% and 0.016%, respectively. Even if the farming would be upscaled to cover the global needs (~1.0×10^6 Mg DW), the ODP-weighted $CHBr_3$ emissions would only increase to 75 Mg and 195 Mg for farming in GTY (GTY_O60_30x) and Darwin (Darwin_O60_30x), respectively. Thus produced $CHBr_3$ would increase the current contribution of $CHBr_3$ to stratospheric ozone depletion by 0.19% and 0.48%, which is again a very small contribution.

To assess the increase of the ODP-weighted $CHBr_3$ emissions under the most extreme and implausible conditions, we envision the total harvest of one year, which contains 752 Mg (21.7

mg $CHBr_3$/g DW*34674 Mg DW) $CHBr_3$, stored in a warehouse of 50 x 25 x 5 m in either of the four locations. We assume that the facility is destroyed, and all 750 Mg released to the atmosphere. Then maximum ODP-weighted $CHBr_3$ emissions would occur for the release in Darwin during January and amount to 215.9 Mg almost doubling the ODP-weighted coastal $CHBr_3$ emissions of Australia. If the entire content of ~1.0×10^6 Mg *Asparagopsis* DW (21.7 mg $CHBr_3$/g DW*1040220 Mg DW=22573 Mg $CHBr_3$) would be released in Darwin, the additional contribution of $CHBr_3$ to global ozone depletion could reach 16%.

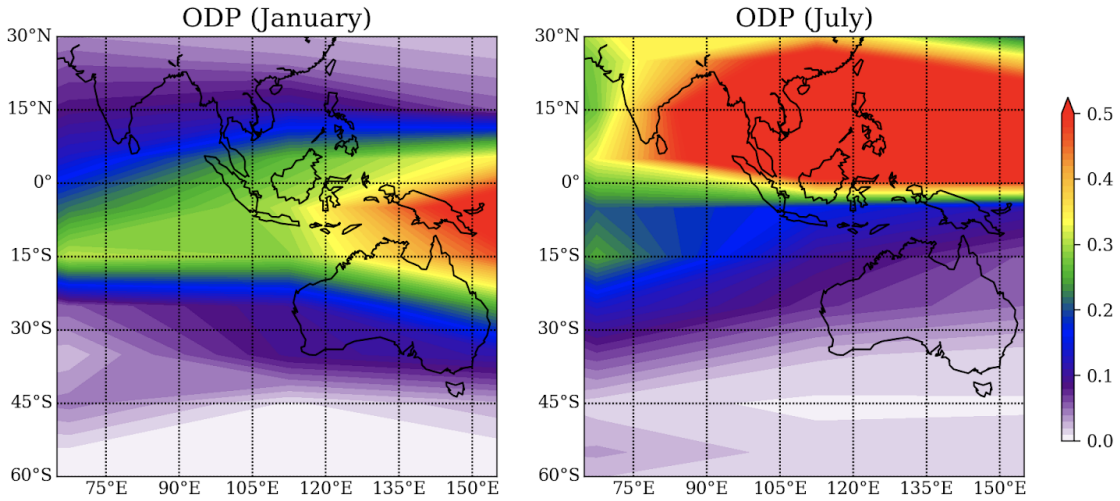

Figure 7. Spatial distribution of the ODP in January and July from Pisso et al. (2010), plotted with interval of 0.01.

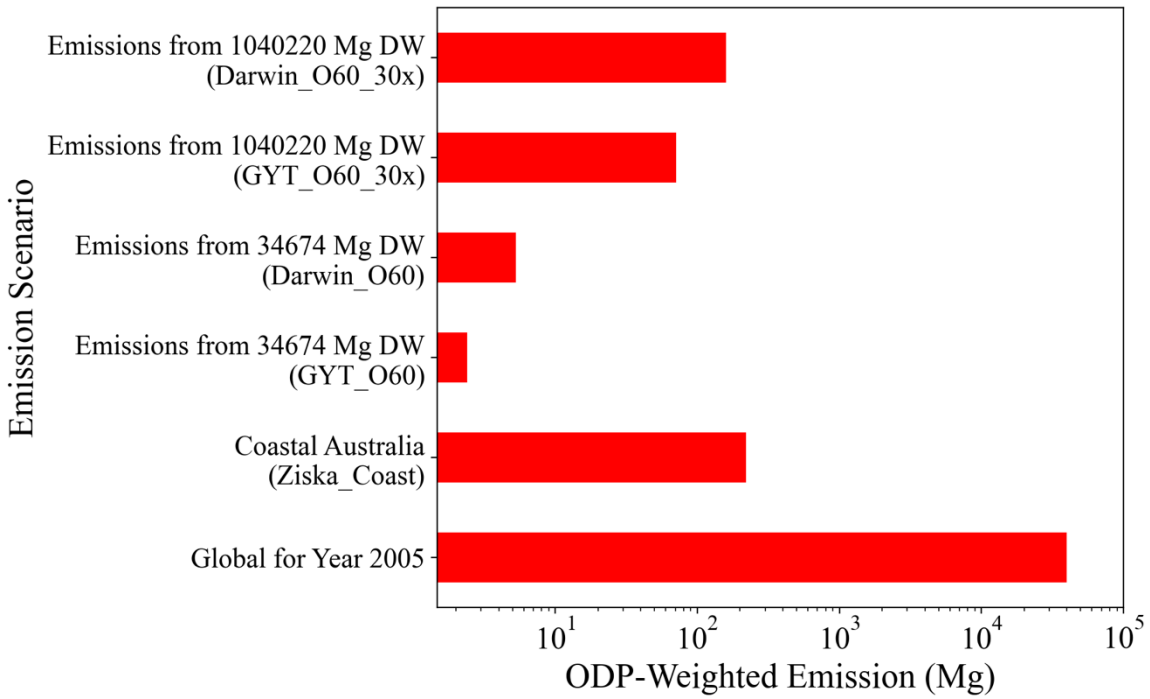

Figure 8. The ODP-weighted emissions of $CHBr_3$ for Global Scenarios (GTY_O60_30x and Darwin_O60_30x), Australian Scenarios (GTY_O60 and Darwin_O60), Coastal Australian emission (Ziska_Coast), and global ODP-weighted emission for 2005 taken from Tegtmeier et al. (2015) as a reference, note that the x-axis is exponential.

5. Summary and Conclusions

In this study, we assessed the potential risks of $CHBr_3$ released from *Asparagopsis* farming near Australia for the stratospheric ozone layer by analyzing different cultivation scenarios. We conclude that the intended operation of *Asparagopsis* seaweed cultivation farms with an annual yield of 34674 Mg DW in either open ocean or terrestrial cultures at the locations Triubanna, Yamba, Geraldton, and Darwin will not impact the ozone layer under normal operating conditions. For Australia scenarios with an annual yield of ~3.5×10^4 Mg DW and algae growth rate of 5% per day, the expected annual $CHBr_3$ emission from the considered *Asparagopsis* farms into the atmosphere (~27 Mg, 0.11 Mmol) is less than 0.9% of the coastal Australian emissions (~3109 Mg, 12.3 Mmol). This contribution is negligible from a global perspective by adding less than 0.01% to the worldwide $CHBr_3$ emissions from natural and anthropogenic sources. The overall emissions from the farms would be even smaller with a faster growth rate for the same annual

yield. We have assumed a high $CHBr_3$ production of 21.7 mg/g DW from superior strains and expected lower $CHBr_3$ production of 14 mg/g DW would likewise reduce emissions to the atmosphere.

The $CHBr_3$ emissions from the localized *Asparagopsis* farms could be larger than emissions from coastal Australia. However, the overall atmospheric impact of the *Asparagopsis* farms is negligible, as the $CHBr_3$ dilutes rapidly and degrades in the atmosphere under normal weather conditions. Mixing ratios of $CHBr_3$ are generally dominated by the coastal Australian emissions. In global scenarios with annual yield ~1.0 $\times 10^6$ Mg DW, localized $CHBr_3$ mixing ratios comparable to the background values can be found in the lower troposphere. In the upper troposphere, on the other hand, mixing ratios larger than background values only appear in the global tropical scenario (Darwin_O60 _30x). The release of the complete $CHBr_3$ content from the macroalgae to the environment on very short timescales (e.g., days) due to extreme weather situations could contribute significant amounts to the atmosphere, especially during times when the standing stock biomass is relatively large (Geraldton_Ex96). While such extreme scenarios could lead to much larger mixing ratios than background values, such mass release events are implausible because even if a farm was totally destroyed the seaweed stock could not instantaneously release all the accumulated $CHBr_3$. Such scenarios have been included here to evaluate a catastrophic and likely impossible worst-case scenario.

The impact of $CHBr_3$ from the proposed seaweed farms on the stratospheric ozone layer is assessed by weighting the emissions with the ozone depletion potential of $CHBr_3$. In total, Australia scenarios could lead to additional ODP-weighted $CHBr_3$ emissions of up to 2.53 Mg per year with farms located in Geraldton, Triubana and Yamba. With all farming performed in Darwin (Darwin_O60), the emitted $CHBr_3$ could reach the stratosphere on shorter time scales and ODP-weighted emissions would increase to 6.48 Mg, which is less than 0.02% of the global ODP-weighted emissions. For global tropical scenario (Darwin_O60_30x), the ODP-weighted emissions amount to 175 Mg, increasing the global ozone depletion by 0.48%, resulting in a very small contribution. The ODP used in this study, does not include the impact of VSLS product gases. Previous modelling studies have highlighted the role of product gas treatment and their impact on the stratospheric halogen budget (e.g., Fernandez et al., 2021). Including product gas entrainment can lead to up to 30% larger ODP values for $CHBr_3$ (Engel and Rigby et al., 2018; Tegtmeier et al., 2020), thus the ODP-weighted emissions presented here can be up to 30% larger.

However, this does not affect our assessment of the potential importance of cultivation induced $CHBr_3$ as the ratios of the impact of each scenario compared with the global ODP-weighted emission remain the same. Another point to note is that Ziska emission potentially underestimate background levels of $CHBr_3$ in coastal regions (Ziska et al., 2013), e.g. $CHBr_3$ measurement in Cape Grim, which is close to Triabunna, shows much larger $CHBr_3$ mixing ratio (~1.5 ppt, Dunse et al., 2020). However, including such higher atmospheric background values in the Ziska methodology would not really increase the fluxes as the flux is driven by air-sea gradient (Eq. 3). Our conclusions will still hold if stronger coastal emission is applied, as it will increase the background $CHBr_3$ mixing ratios.

We note that all data characterizing the potential systems for the production of *Asparagopsis* are based on few available literature data, laboratory scale tests and relatively small-scale field trials. This not only places limitations on the technological representativeness of a future system and the temporal validity of the study, but also demonstrates importance for directed studies, especially on the release of $CHBr_3$ from *Asparagopsis* during cultivation. As this understanding evolves so will the cultivation and processing technologies engineered to conserve the antimethanogenic $CHBr_3$ in the seaweed biomass which is the primary value feature of *Asparagopsis*. These limitations are largely mitigated in our study by evaluating various environmental and meteorological conditions ranging from conservative to most extreme scenarios and by investigating different farming practices based on various sensitivity studies.

Data availability

The $CHBr_3$ emission data and FLEXPART output can be obtained from the authors on request via BQ (bquack@geomar.de), ST (susann.tegtmeier@usask.ca), or YJ (yue.jia@noaa.gov).

Author Contributions

BQ initialized the idea. YJ, BQ, and ST carried out the calculations and analysis. YJ performed the FLEXPART simulations and produced the figures. YJ, BQ, and ST wrote the manuscript with the contribution from other co-authors RK and IP. RK contributed to conceptualization, design, writing, editing, procurement of funding. All the authors contributed to discussions and revisions of the manuscript.

Competing interests

The authors declare that they have no conflict of interest.

Acknowledgements

The authors wish to acknowledge CSIRO, FutureFeed, and Sea Forest for their provision of technical knowledge, data, and insight into Asparagopsis supply chains in Australia. The authors would like to thank the European Centre for Medium-Range Weather Forecasts (ECMWF) for the ERA-Interim reanalysis data and the FLEXPART development team for the Lagrangian particle dispersion model used in this publication. The FLEXPART simulations were performed on resources provided by the University of Saskatchewan.

Reference

Abbott, D. W., Aasen, I. M., Beauchemin, K. A., Grondahl, F., Gruninger, R., Hayes, M., Huws, S., Kenny, D. A., Krizsan, S. J., Kirwan, S. F., Lind, V., Meyer, U., Ramin, M., Theodoridou, K., von Soosten, D., Walsh, P. J., Waters, S., and Xing, X.: Seaweed and Seaweed Bioactives for Mitigation of Enteric Methane: Challenges and Opportunities, Animals, 10, 2432, https://doi.org/10.3390/ani10122432, 2020.

Aschmann, J., Sinnhuber, B. M., Atlas, E. L., and Schauffler, S. M.: Modeling the transport of very short-lived substances into the tropical upper troposphere and lower stratosphere, Atmos. Chem. Phys., 9, 9237-9247, 10.5194/acp-9-9237-2009, 2009.

Battaglia, M. CSIRO and FutureFeed Pty Ltd. Personal Communication. 2020. https://www.csiro.au/ and https://www.future-feed.com/

Beauchemin, K. A., Ungerfeld, E. M., Eckard, R. J., and Wang, M.: Review: Fifty years of research on rumen methanogenesis: lessons learned and future challenges for mitigation, Animals, 14, S2-S16, https://doi.org/10.1017/S1751731119003100, 2020.

Black, J. L., Davison, T. M., Box, I.: Methane Emissions from Ruminants in Australia: Mitigation Potential and Applicability of Mitigation Strategies. Animals, 11, 951. https://doi.org/10.3390/ani11040951, 2021

Brioude, J., Portmann, R. W., Daniel, J. S., Cooper, O. R., Frost, G. J., Rosenlof, K. H., Granier, C., Ravishankara, A. R., Montzka, S. A., and Stohl, A.: Variations in ozone depletion potentials of very short-lived substances with season and emission region, Geophysical Research Letters, 37, https://doi.org/10.1029/2010GL044856, 2010.

Burreson, B. J., Moore, R. E., and Roller, P. P.: Volatile halogen compounds in the alga Asparagopsis taxiformis (Rhodophyta), Journal of Agricultural and Food Chemistry, 24, 856-861, 10.1021/jf60206a040, 1976.

Carpenter, L. J., and Liss, P. S.: On temperate sources of bromoform and other reactive organic bromine gases, Journal of Geophysical Research: Atmospheres, 105, 20539-20547, https://doi.org/10.1029/2000JD900242, 2000.

Carpenter, L. J., Reimann, S. (Lead Authors), Burkholder, J. B., Clerbaux, C., Hall, B. D., and Hossaini, R.: Ozone-depleting substances (ODSs) and other gases of interest to the Montreal Protocol. In: Scientific assessment of ozone depletion: 2014. Global Ozone Research and Monitoring Project-Report A., E. and A., M. S. (Eds.), World Meteorological Organization., Geneva, Switzerland, 2014.

Claxton, T., R. Hossaini, O. Wild, M.P. Chipperfield, and C. Wilson, On the regional and seasonal ozone depletion potential of chlorinated very shortlived substances, Geophys. Res. Lett., 46(10), 5489–5498. doi:10.1029/2018GL081455, 2019.

Dee, D. P., Uppala, S. M., Simmons, A. J., Berrisford, P., Poli, P., Kobayashi, S., Andrae, U., Balmaseda, M. A., Balsamo, G., Bauer, P., Bechtold, P., Beljaars, A. C. M., van de Berg, L., Bidlot, J., Bormann, N., Delsol, C., Dragani, R., Fuentes, M., Geer, A. J., Haimberger, L., Healy, S. B., Hersbach, H., Holm, E. V., Isaksen, L., Kallberg, P., Kohler, M., Matricardi, M., McNally, A. P., Monge-Sanz, B. M., Morcrette, J. J., Park, B. K., Peubey, C., de Rosnay, P., Tavolato, C., Thepaut, J. N., and Vitart, F.: The ERA-Interim reanalysis: configuration and performance of the data assimilation system, Q J Roy Meteor Soc, 137, 553-597, https://doi.org/10.1002/qj.828, 2011.

Dunse, B. L., Derek, N., Fraser, P. J., Krummel, P. B., and Steele, L. P.: Australian and Global Emissions of Ozone Depleting Substances, Report prepared for the Australian Government Department of Agriculture, Water and the Environment, CSIRO Oceans and Atmosphere, Climate Science Centre, Melbourne, Australia, viii, 58 p., 2020.

Elsom, S. Sea Forest Asparagopsis production. Personal Communication. https://www.seaforest.com.au/, 2020.

Engel, A., and Rigby, M. (Lead Authors), Burkholder, J. B., Fernandez, R. P., Froidevaux, L., Hall, B. D., Hossaini, R., Saito, T., Vollmer, M. K., and Yao, B.: Update on Ozone-Depleting Substances (ODSs) and Other Gases of Interest to the Montreal Protocol, Chapter 1 in Scientific Assessment of Ozone Depletion: 2018, Global Ozone Research and Monitoring Project — Report No. 58, World Meteorological Organization, Geneva, Switzerland, 2018.

Fernandez, R. P., Barrera, J. A., López-Noreña, A. I., Kinnison, D. E., Nicely, J., Salawitch, R. J., Wales, P. A., Toselli, B. M., Tilmes, S., Lamarque, J.-F., Cuevas, C. A., and Saiz-Lopez, A.: Intercomparison between surrogate, explicit and full treatments of VSL bromine chemistry within the CAM-Chem chemistry-climate model. Geophysical Research Letters, 48, e2020GL091125. https://doi.org/10.1029/2020GL091125, 2021.

Forster, C., Stohl, A., and Seibert, P.: Parameterization of Convective Transport in a Lagrangian Particle Dispersion Model and Its Evaluation, Journal of Applied Meteorology and Climatology, 46, 403-422, 10.1175/jam2470.1, 2007.

Gerber, P.J., Steinfeld, H., Henderson, B., Mottet, A., Opio, C., Dijkman, J., Falcucci, A. & Tempio, G.: Tackling climate change through livestock – A global assessment of emissions and mitigation opportunities. Food and Agriculture Organization of the United Nations (FAO), Rome, 2013.

Hense, I., and Quack, B.: Modelling the vertical distribution of bromoform in the upper water column of the tropical Atlantic Ocean, Biogeosciences, 6, 535-544, 10.5194/bg-6-535-2009, 2009.

Herrero, M., and Thornton, P. K.: Livestock and global change: Emerging issues for sustainable food systems, Proceedings of the National Academy of Sciences, 110, 20878-20881, 10.1073/pnas.1321844111, 2013.

Hossaini, R., Chipperfield, M. P., Monge-Sanz, B. M., Richards, N. A. D., Atlas, E., and Blake, D. R.: Bromoform and dibromomethane in the tropics: a 3-D model study of chemistry and transport, Atmos. Chem. Phys., 10, 719-735, 10.5194/acp-10-719-2010, 2010.

Hung, L. D., Hori, K., Nang, H. Q., Kha, T., and Hoa, L. T.: Seasonal changes in growth rate, carrageenan yield and lectin content in the red alga Kappaphycus alvarezii cultivated in Camranh Bay, Vietnam, Journal of Applied Phycology, 21, 265-272, 10.1007/s10811-008-9360-2, 2009.

IPCC: Climate Change 2022: The Physical Science Basis. Contribution of Working Groups I to the Sixth Assessment Report of the Intergovernmental Panel on Climate Change IPCC, Geneva, Switzerland, 2021.

Kamra, D. N.: Rumen microbial ecosystem, Curr Sci India, 89, 124-135, http://www.jstor.org/stable/24110438, 2005.

Kinley, R. D. and Fredeen, A. H.: In Vitro Evaluation of Feeding North Atlantic Stormtoss Seaweeds on Ruminal Digestion. Journal of Applied Phycology, 27, 2387 2393. http://dx.doi.org/10.1007/s10811-014-0487-z, 2015.

Kinley, R., Vucko, M., Machado, L., and Tomkins, N.: In Vitro Evaluation of the Antimethanogenic Potency and Effects on Fermentation of Individual and Combinations of Marine Macroalgae. American Journal of Plant Sciences, 7, 2038-2054. doi: 10.4236/ajps.2016.714184, 2016a.

Kinley, R. D., de Nys, R., Vucko, M. J., Machado, L., and Tomkins, N. W.: The red macroalgae *Asparagopsis taxiformis* is a potent natural antimethanogenic that reduces methane production during *in vitro* fermentation with rumen fluid, Animal Production Science, 56, 282-289, https://doi.org/10.1071/AN15576, 2016b.

Kinley, R. D., Martinez-Fernandez, G., Matthews, M. K., de Nys, R., Magnusson, M., and Tomkins, N. W.: Mitigating the carbon footprint and improving productivity of ruminant livestock agriculture using a red seaweed, Journal of Cleaner Production, 259, 120836, https://doi.org/10.1016/j.jclepro.2020.120836, 2020.

Leedham, E. C., Hughes, C., Keng, F. S. L., Phang, S. M., Malin, G., and Sturges, W. T.: Emission of atmospherically significant halocarbons by naturally occurring and farmed tropical macroalgae, Biogeosciences, 10, 3615-3633, 10.5194/bg-10-3615-2013, 2013.

Li, X. X., Norman, H. C., Kinley, R. D., Laurence, M., Wilmot, M., Bender, H., de Nys, R., and Tomkins, N.: Asparagopsis taxiformis decreases enteric methane production from sheep, Animal Production Science, 58, 681-688, https://doi.org/10.1071/AN15883, 2018.

Liang, Q., Stolarski, R. S., Kawa, S. R., Nielsen, J. E., Douglass, A. R., Rodriguez, J. M., Blake, D. R., Atlas, E. L., and Ott, L. E.: Finding the missing stratospheric Br_y: a global modeling study of CHBr₃ and CH₂Br₂, Atmos. Chem. Phys., 10, 2269-2286, 10.5194/acp-10-2269-2010, 2010.

Maas, J., Tegtmeier, S., Quack, B., Biastoch, A., Durgadoo, J. V., Ruhs, S., Gollasch, S., and David, M.: Simulating the spread of disinfection by-products and anthropogenic bromoform emissions from ballast water discharge in Southeast Asia, Ocean Sci, 15, 891-904, 10.5194/os-15-891-2019, 2019.

Maas, J., Tegtmeier, S., Jia, Y., Quack, B., Durgadoo, J. V., and Biastoch, A.: Simulations of anthropogenic bromoform indicate high emissions at the coast of East Asia, Atmos. Chem. Phys., 21, 4103-4121, 10.5194/acp-21-4103-2021, 2021.

Machado, L., Magnusson, M., Paul, N. A., de Nys, R., and Tomkins, N.: Effects of Marine and Freshwater Macroalgae on In Vitro Total Gas and Methane Production, PLOS ONE, 9, e85289, 10.1371/journal.pone.0085289, 2014.

Machado, L., Magnusson, M., Paul, N. A., Kinley, R., de Nys, R., and Tomkins, N. W.: Identification of bioactives from the red seaweed Asparagopsis taxiformis that promote antimethanogenic activity in vitro, J. Appl. Phycol., 28, 3117-3126, https://doi.org/10.1007/s10811-016-0830-7, 2016.

Magnusson, M., Vucko, M. J., Neoh, T. L., and de Nys, R.: Using oil immersion to deliver a naturally-derived, stable bromoform product from the red seaweed Asparagopsis taxiformis, Algal Research, 51, 102065, https://doi.org/10.1016/j.algal.2020.102065, 2020.

Marshall, R. A., Harper, D. B., McRoberts, W. C., and Dring, M. J.: Volatile bromocarbons produced by Falkenbergia stages of Asparagopsis spp. (Rhodophyta), Limnology and Oceanography, 44, 1348-1352, doi: 10.4319/lo.1999.44.5.1348, 1999.

Mata, L., Gaspar, H., and Santos, R.: CARBON/NUTRIENT BALANCE IN RELATION TO BIOMASS PRODUCTION AND HALOGENATED COMPOUND CONTENT IN THE RED ALGA ASPARAGOPSIS TAXIFORMIS (BONNEMAISONIACEAE)1, Journal of Phycology, 48, 248-253, https://doi.org/10.1111/j.1529-8817.2011.01083.x, 2012.

Mata, L., Lawton, R. J., Magnusson, M., Andreakis, N., de Nys, R., and Paul, N. A.: Within-species and temperature-related variation in the growth and natural products of the red alga Asparagopsis taxiformis, Journal of Applied Phycology, 29, 1437-1447, 10.1007/s10811-016-1017-y, 2017.

Mayberry, D., Bartlett, H., Moss, J., Davison, T., and Herrero, M.: Pathways to carbon-neutrality for the Australian red meat sector, Agricultural Systems, 175, 13-21, https://doi.org/10.1016/j.agsy.2019.05.009, 2019.

Moate, P. J., Deighton, M. H., Williams, S. R. O., Pryce, J. E., Hayes, B. J., Jacobs, J. L., Eckard, R. J., Hannah, M. C., and Wales, W. J.: Reducing the carbon footprint of Australian milk production by mitigation of enteric methane emissions, Animal Production Science, 56, 1017-1034, https://doi.org/10.1071/AN15222, 2016.

Moore, R. M., Geen, C. E., and Tait, V. K.: Determination of Henry's Law constants for a suite of naturally occurring halogenated methanes in seawater, Chemosphere, 30, 1183-1191, https://doi.org/10.1016/0045-6535(95)00009-W, 1995a.

Moore, R. M., Tokarczyk, R., Tait, V. K., Poulin, M., and Geen, C.: Marine phytoplankton as a natural source of volatile organohalogens. In: Naturally-Produced Organohalogens, Grimvall, A. and de Leer, E. W. B. (Eds.), Springer Netherlands, Dordrecht, 1995b.

Morgavi, D. P., Forano, E., Martin, C., and Newbold, C. J.: Microbial ecosystem and methanogenesis in ruminants, Animal, 4, 1024-1036, 10.1017/s1751731110000546, 2010.

Montzka, S. A. and Reimann, S. et al.: Ozone-depleting substances andrelated chemicals, in Scientific Assessment of Ozone Depletion:2010, Global Ozone Research and Monitoring Project – ReportNo. 52, WMO, Geneva, Switzerland, 2011.

Nightingale, P. D., Malin, G., and Liss, P. S.: Production of chloroform and other low molecular-weight halocarbons by some species of macroalgae, Limnology and Oceanography, 40, 680-689, https://doi.org/10.4319/lo.1995.40.4.0680, 1995.

Nightingale, P. D., Malin, G., Law, C. S., Watson, A. J., Liss, P. S., Liddicoat, M. I., Boutin, J., and Upstill-Goddard, R. C.: In situ evaluation of air-sea gas exchange parameterizations using novel conservative and volatile tracers, Global Biogeochemical Cycles, 14, 373-387, https://doi.org/10.1029/1999GB900091, 2000.

Patra, A. K.: Enteric methane mitigation technologies for ruminant livestock: a synthesis of current research and future directions, Environ Monit Assess, 184, 1929-1952, 10.1007/s10661-011-2090-y, 2012.

Paul, N. A., de Nys, R., and Steinberg, P. D.: Chemical defence against bacteria in the red alga Asparagopsis armata: linking structure with function, Marine Ecology Progress Series, 306, 87-101, 10.3354/meps306087, 2006.

Pisso, I., Haynes, P. H., and Law, K. S.: Emission location dependent ozone depletion potentials for very short-lived halogenated species, Atmos. Chem. Phys., 10, 12025-12036, 10.5194/acp-10-12025-2010, 2010.

Pisso, I., Sollum, E., Grythe, H., Kristiansen, N. I., Cassiani, M., Eckhardt, S., Arnold, D., Morton, D., Thompson, R. L., Groot Zwaaftink, C. D., Evangeliou, N., Sodemann, H., Haimberger, L., Henne, S., Brunner, D., Burkhart, J. F., Fouilloux, A., Brioude, J., Philipp, A., Seibert, P., and Stohl, A.: The Lagrangian particle dispersion model FLEXPART version 10.4, Geosci. Model Dev., 12, 4955-4997, 10.5194/gmd-12-4955-2019, 2019.

Quack, B., and Wallace, D. W. R.: Air-sea flux of bromoform: Controls, rates, and implications, Global Biogeochemical Cycles, 17, https://doi.org/10.1029/2002GB001890, 2003.

Roque, B. M., Venegas, M., Kinley, R. D., de Nys, R., Duarte, T. L., Yang, X., and Kebreab, E.: Red seaweed (Asparagopsis taxiformis) supplementation reduces enteric methane by over 80 percent in beef steers, PLOS ONE, 16, e0247820, 10.1371/journal.pone.0247820, 2021.

Sinnhuber, B.-M., and Meul, S.: Simulating the impact of emissions of brominated very short lived substances on past stratospheric ozone trends, Geophysical Research Letters, 42, 2449-2456, https://doi.org/10.1002/2014GL062975, 2015.

Stohl, A., Hittenberger, M., and Wotawa, G.: Validation of the lagrangian particle dispersion model FLEXPART against large-scale tracer experiment data, Atmospheric Environment, 32, 4245-4264, https://doi.org/10.1016/S1352-2310(98)00184-8, 1998.

Stohl, A. and Thomson, D.: A density correction for Lagrangian particle dispersion models, Boundary-Layer Meteorology, 90, 155-167, 10.1023/A:1001741110696, 1999.

Stohl, A. and Trickl, T.: A textbook example of long-range transport: Simultaneous observation of ozone maxima of stratospheric and North American origin in the free troposphere over Europe, Journal of Geophysical Research: Atmospheres, 104, 30445-30462, 10.1029/1999JD900803,1999.

Tegtmeier, S., Ziska, F., Pisso, I., Quack, B., Velders, G. J. M., Yang, X., and Krüger, K.: Oceanic bromoform emissions weighted by their ozone depletion potential, Atmos. Chem. Phys., 15, 13647-13663, 10.5194/acp-15-13647-2015, 2015.

Tegtmeier, S., Atlas, E., Quack, B., Ziska, F., and Krüger, K.: Variability and past long-term changes of brominated very short-lived substances at the tropical tropopause, Atmos. Chem. Phys., 20, 7103-7123, 10.5194/acp-20-7103-2020, 2020.

Vucko, M. J., Magnusson, M., Kinley, R. D., Villart, C., and de Nys, R.: The effects of processing on the in vitro antimethanogenic capacity and concentration of secondary metabolites of Asparagopsis taxiformis, J. Appl. Phycol., 29, 1577-1586, 10.1007/s10811-016-1004-3, 2017.

Wuebbles, D. J.: Chlorocarbon Emission Scenarios - Potential Impact on Stratospheric Ozone, Journal of Geophysical Research-Oceans, 88, 1433-1443, 10.1029/JC088iC02p01433, 1983.

Yang, X., Abraham, N. L., Archibald, A. T., Braesicke, P., Keeble, J., Telford, P. J., Warwick, N. J., and Pyle, J. A.: How sensitive is the recovery of stratospheric ozone to changes in concentrations of very short-lived bromocarbons?, Atmospheric Chemistry and Physics, 14, 10431-10438, 10.5194/acp-14-10431-2014, 2014.

Yong, Y. S., Yong, W. T. L., and Anton, A.: Analysis of formulae for determination of seaweed growth rate, Journal of Applied Phycology, 25, 1831-1834, 10.1007/s10811-013-0022-7, 2013.

Zhang, J., Wuebbles, D. J., Kinnison, D. E., and Saiz-Lopez, A.: Revising the ozone depletion potentials metric for short-lived chemicals such as CF3I and CH3I, J. Geophys. Res. Atmos., 125, e2020JD032414, https://doi.org/10.1029/2020JD032414, 2020.

878 Ziska, F., Quack, B., Abrahamsson, K., Archer, S. D., Atlas, E., Bell, T., Butler, J. H., Carpenter,
879 L. J., Jones, C. E., Harris, N. R. P., Hepach, H., Heumann, K. G., Hughes, C., Kuss, J., Kruger, K.,
880 Liss, P., Moore, R. M., Orlikowska, A., Raimund, S., Reeves, C. E., Reifenhauser, W., Robinson,
881 A. D., Schall, C., Tanhua, T., Tegtmeier, S., Turner, S., Wang, L., Wallace, D., Williams, J.,
882 Yamamoto, H., Yvon-Lewis, S., and Yokouchi, Y.: Global sea-to-air flux climatology for
883 bromoform, dibromomethane and methyl iodide, Atmospheric Chemistry and Physics, 13, 8915-
884 8934, 10.5194/acp-13-8915-2013, 2013.